Research Article Vol. 54, No. 14 / May 10 2015 / Applied Optics 4485

applied optics

Simulation design of a wearable see-through retinal projector

WEN-SHING SUN,[1] CHUEN-LIN TIEN,[2,*] YEN-CHEN CHIANG,[1] AND JUI-WEN PAN[3]

[1]Department of Optics and Photonics, National Central University, 32001 Chungli, Taiwan
[2]Department of Electrical Engineering, Feng Chia University, 40724 Taichung, Taiwan
[3]Institute of Photonic Systems, National Chiao Tung University, Tainan City 71150, Taiwan
*Corresponding author: cltien@fcu.edu.tw

Received 4 December 2014; revised 5 March 2015; accepted 6 April 2015; posted 9 April 2015 (Doc. ID 228325); published 7 May 2015

This study proposes a new simulation design for a wearable see-through retinal projector combined with a compact camera. The see-through retinal projector is composed of an illumination system and eyepiece system. In this eyeglass-mounted design, all the information is projected directly into the user's eyes using a see-through retinal projector. The retinal projector forms a 20 in. (50.8 cm) upright virtual image located 2 m in front of the human eye, and the illumination system provides uniform illumination for liquid crystal on silicon (LCoS) panels. Moreover, an RGB LED array is used as the light source to generate color images with color sequences. The compact camera has a lens with an aperture of F/2.8, a half field-of-view (FOV) of 30°, and 2 million pixels. This optical system design with the combination of a see-through retinal projector and a compact camera has a volume of about 5.83 cm^3 and a weight of 6.02 g.

OCIS codes: (120.4820) Optical systems; (220.2740) Geometric optical design; (220.4298) Nonimaging optics; (220.3620) Lens system design.

http://dx.doi.org/10.1364/AO.54.004485

1. INTRODUCTION

A wearable retinal projector, as a type of head-mounted display, was first proposed and developed in the 1960s by Sutherland [1]. Head-mounted displays were initially applied for military purposes, such as in the helmets of military aircraft pilots [2]. After several decades of development as well as the emergence of new manufacturing technologies and new designs, the applications of head-mounted displays are no longer restricted to the military and have expanded to the fields of medicine, engineering design, education, training, entertainment, and emergency rescue [3–5]. Head-mounted displays can be designed to be monocular or binocular, the former implementing small volume and light mobile screens for guidance and real-time information, and the latter able to show stereoscopic effects by displaying images to both eyes. The usage and mounting are distinct, but there are several common designs features to the optics. Based on the design principles, these devices can be divided into lens- or projection-type. The former type first allowed images to be directly observed on a panel with an ocular lens. The latter type, on the other hand, has been improved from the traditional head-mounted displays by Kijima and Hirosw [6], Fisher [7], and Fergason [8] in the 1990s. They replaced the original ocular lens with a projection lens and changed the traditional scattering projector into a retro-reflector for reflecting light back to the human eye through the original route.

Virtual-reality head-mounted display designs can be either non-see-through or see-through [9]. The differences reside in the simultaneous acquisition of external images, so that the external images and those on the display are simultaneously projected into the eyes when using the head-mounted display. The non-see-through design is utilized for virtual reality displays, while the see-through design is applied for guidance or instruction purposes. The see-through design is further divided into optical see-through and electronic see-through types. The former type is designed to allow the eye to simultaneously view external images and information on the panel (through the use of beam splitters), while the latter acquires external images through a lens on the head-mounted display, which are further shown on the display. The optical see-through design does not stop external images from entering the eye and, therefore, presents better mounting perception [10]. In 2012, Cameron [11] reported on a BAE system that exploited optical waveguide technology to develop the Q-Sight family of scalable helmet mounted displays. The Q-Sight offers monochromatic displays and has a large eye-box. Rolland and Fuchs [12] reviewed several medical visualization applications developed to use optical and video see-through technologies. They reported

1559-128X/15/144485-10$15/0$15.00

on the technological, human factors, and perceptual issues related to see-through devices, some of which were employed in the various applications surveyed. Bauer and Rolland [13] developed two optical see-through head-worn display designs, both comprising two free-form elements with an emphasis on visual space assessment and parameters. This design could not only eliminate color aberration but could also shorten the length of the optical system and lessen its weight, but the changes would have a significant impact on the tolerance.

Changes in display technology and enhancement of mobile communication technology have led to faster information acquisition and more convenience for the user. In addition, advances in manufacturing technology, the appearance of small-scale panels, and the boom in microprojection systems have allowed designers of head-mounted displays to overcome the traditional problems of complex structures, heavy weight, and high costs, leading to further popularizing of these devices for the general consumer market. Head-mounted displays offer advantages of providing instant information with a high-resolution screen while still offering restricted volume and weight, so that the user is able to have empty hands to carry out other tasks and present greater privacy. The display systems will be critical in the next generation of devices. In this work, we propose a wearable see-through retinal projector that offers full color display with a small eye-box. With these advantages, our design provides the potential user with a low-cost product that is easy to operate, compact, and lightweight.

2. OPTICAL DESIGN OF A SEE-THROUGH RETINAL PROJECTOR

The optical design of our see-through retinal projector includes an eyepiece system and an illumination system, as shown in Fig. 1, where a microprojector structure is utilized for lightening the liquid crystal on silicon (LCoS) panel [14], allowing the user to see through the eyepiece system, with a beam splitter (BS). The eyepiece system is combined with a polarizing beam splitter (PBS) and a BS, which function to show the images on the LCoS panel as an object, so that human eye can directly view the images on the display. In this case, a screen is not necessary as is generally used in projection systems. Moreover, the BS is used to combine the external images and the ones on the panel to simply achieve the "see-through" effect. The PBS is a beam combined with an eyepiece system and an illumination system that aims to provide efficient and uniform luminance on the panel. For weight and volume considerations, an RGB LED array is used as the light source. A collimator and lens array system are utilized to ensure high uniformity of the illumination system. A color sequential display is applied to present different colors for the LCoS panel. The optical camera system has a camera lens with the aperture of F/2.8, a half field-of-view (FOV) of 30°, and a resolution of 2 million pixels. The camera system allows acquisition of external images for identification, further providing users with real-time information, recording capability, and the capacity of taking pictures.

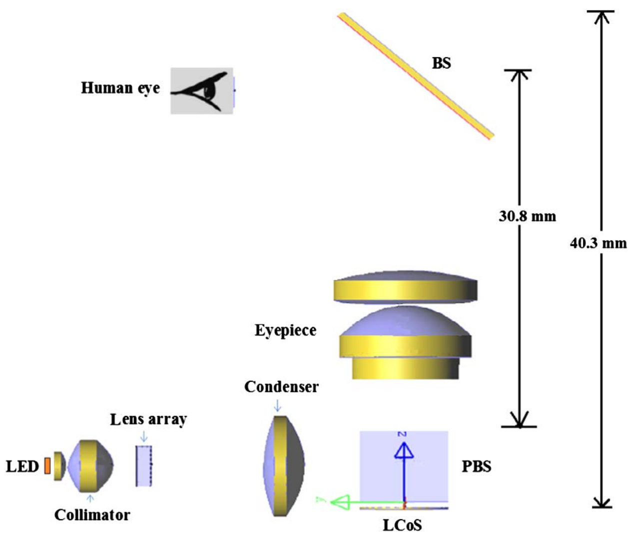

Fig. 1. Schematic of the retinal projector system.

3. DESIGN RESULTS OF THE EYEPIECE SYSTEM

The eyepiece system for the retinal projector forms a 20 in. (50.8 cm) upright virtual image located 2 m in front of the human eye. The first-order specifications should be determined before designing the eyepiece system. Since this is an optical system for human users, the characteristics of the human eye need to be taken into account. The composition of the eyepiece system is divided into four parts, as illustrated in Fig. 2. The display panel acts as the light valve of the system to provide the display information; LCoS panels are selected for this design. The PBS aims to combine the eyepiece and illumination systems. The eyepiece governs the movement of projected images on the panel into the human eye; three pieces of plastic material are used for this design. The BS is utilized to combine the external images and the images on the eyepiece, so that the eye could simultaneously receive both images.

A. Display Panel Selection

Most optical parameters are affected by the selection of panels, such as the volume and weight of the system. In order to design a lightweight system, a 0.177 in. (0.44958 cm) LCoS panel (HOLOEYE) is selected, and the panel resolution is 640 × 480

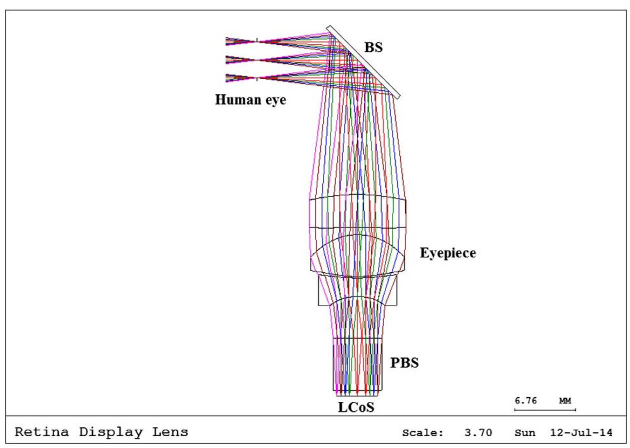

Fig. 2. Eyepiece system layout.

VGA (specifications are shown in Table 1). For a color sequential display, the designed LCoS panel demonstrates a frame rate of 180 Hz, an aperture ratio larger than 88%, a reflectance of 53%, and a weight of 3.50 g.

B. First-Order Specifications of the Eyepiece System

The first-order specifications of the eyepiece system should be calculated by taking into consideration the characteristics of the human eye, as shown in Table 2. In the eyepiece system, the panel is regarded as an object in the image. An enlarged virtual image is projected 2 m in front of the eyes through the eyepiece. Because the LCoS pixel pitch is 5.625 μm and the projection magnification through the eyepiece system is 113, a single pixel on the LCoS is projected to a 2 m distance with a width of 0.635 mm, corresponding to the human eye being able to see a resolution of 1.1 arc min. The projection distance is set to 2 m in front of the eye, the half FOV is 7.125°, the exit pupil diameter is 4 mm, and the eye relief is 10 mm, which is the distance between the eye and the beam splitter.

C. Design Results and Tolerance Analysis

The eyepiece system forms a virtual image in front of the LCoS. The image distance is 2 m from the eyepiece to the virtual image position. It has a magnifying function with a magnification of 113. The eyepiece system is composed of a PBS, an eyepiece, and a BS, as shown in Fig. 2. The optical quality of the system is shown in Fig. 3. Figure 3(a) shows the spatial frequency and the modulation transfer function (MTF) curves for a half FOV from 0° to 7.125°. For an LCoS pixel size of 5.625 μm, we select a maximum spatial frequency of 90 lp/mm. The MTF value is larger than 60% at a frequency of 90 lp/mm.

Table 1. LCoS Specifications

Description	Specifications
Display type	Reflective LCoS
Dynamic range	8 bits per color
Resolution	640 × 480 (VGA)
Device diagonal	0.177 in. (0.44958 cm)
Active area	3.6 × 2.7 mm
Aperture ratio	>88%
Pixel pitch	5.625 μm
Frame rate	180 Hz
Reflectance	53%
Weight	3.50 g
Operating Waveband	420–700 nm
Lifetime	>20.000 h

Table 2. First-Order Data of the Image System

Specifications	Value
Half diagonal (LCoS)	2.25 mm
Image distance	–2000 mm
Image resolution for eye	1.1 arc min
Half FOV	7.125°
EFL	18 mm
Exit pupil diameter	4 mm
Image NA	0.111
Eye relief	10 mm
Lens type	Telecentric for image space

Figure 3(b) illustrates the relation between the lateral color and the FOV. The red line indicates the longitudinal chromatic aberration curve from 465.61 to 642.73 nm, which has a maximum value of 3.02 μm. The green line is the longitudinal chromatic aberration curve from 465.61 to 542.02 nm, which has a maximum value of 5.60 μm. These values are less than 1 pixel size of 5.625 μm. Since the resolution of the human eyes is less than 1.1 arcmin, so the lateral chromatic aberration is difficult to observe. Figure 3(c) shows the distortion and the astigmatic field curves, where the maximal distortion is 0.98%. The TV distortion is 0.63%, which is the difference between two distortion fields of view, 0.6 and 1.0. Figure 3(d) presents the results of tolerance analysis, in which the tolerance MTF curves of all fields of view are larger than 31% at 90 lp/mm when the cumulative probability is 97.7%.

4. DESIGN RESULTS FOR THE ILLUMINATION SYSTEM

The structure of the illumination system for the retinal projector is illustrated in Fig. 4. In this design, a lens array with a collimator and a condenser is used as the light uniform element. In addition, the LED and the color sequence are used to achieve uniformity and color mixing in a simple optomechanical system. Specifications and design of the elements are introduced below.

A. Specifications of the Light Source

The LED used is the 20 million chip produced by OSRAM. The arrangement and the specifications of the LEDs are shown in Fig. 5 and Table 3. The device is composed of a red, blue, and two green LED chips with an emission area of 0.5 mm × 0.5 mm to make a total area of 1 mm × 1 mm. The LED light source module could be simplified with the incorporation of a common collimator.

B. Design of the Collimator

The LED is designed as the object focus on the collimator so that the light source is aligned through the collimator with parallel beams from various beam angles. When the diagonal height h_{LED} of the LED and the maximal emission angle θ_{mlain} are known, the focus of the collimator $f_{collimator}$ is expressed as

$$\tan\theta_{mlain} = \frac{h_{LED}}{f_{collimator}}. \tag{1}$$

To design the collimator for an object-space telecentric system, the first array lens is located at the focal point of the collimator, and the position of the exit pupil overlaps the incident surface of the lens array, so that all collected beams can enter the lens array, as shown in Fig. 6.

C. Design of the Lens Array

The lens array is composed of some lens units with a rectangular external diameter, as illustrated in Fig. 7(a). The aspect ratio should be the same as the illumination area. The first and the second surfaces are mutual focal planes, and the thickness (L_{mia}) of the lens unit is the focal length (f_{s1}) of the first surface, to achieve the uniformity effect. The incident beam enters the first surface with a maximum angle θ_{mlain}, as shown in Fig. 7(b). If a certain height of the second surface is imaged

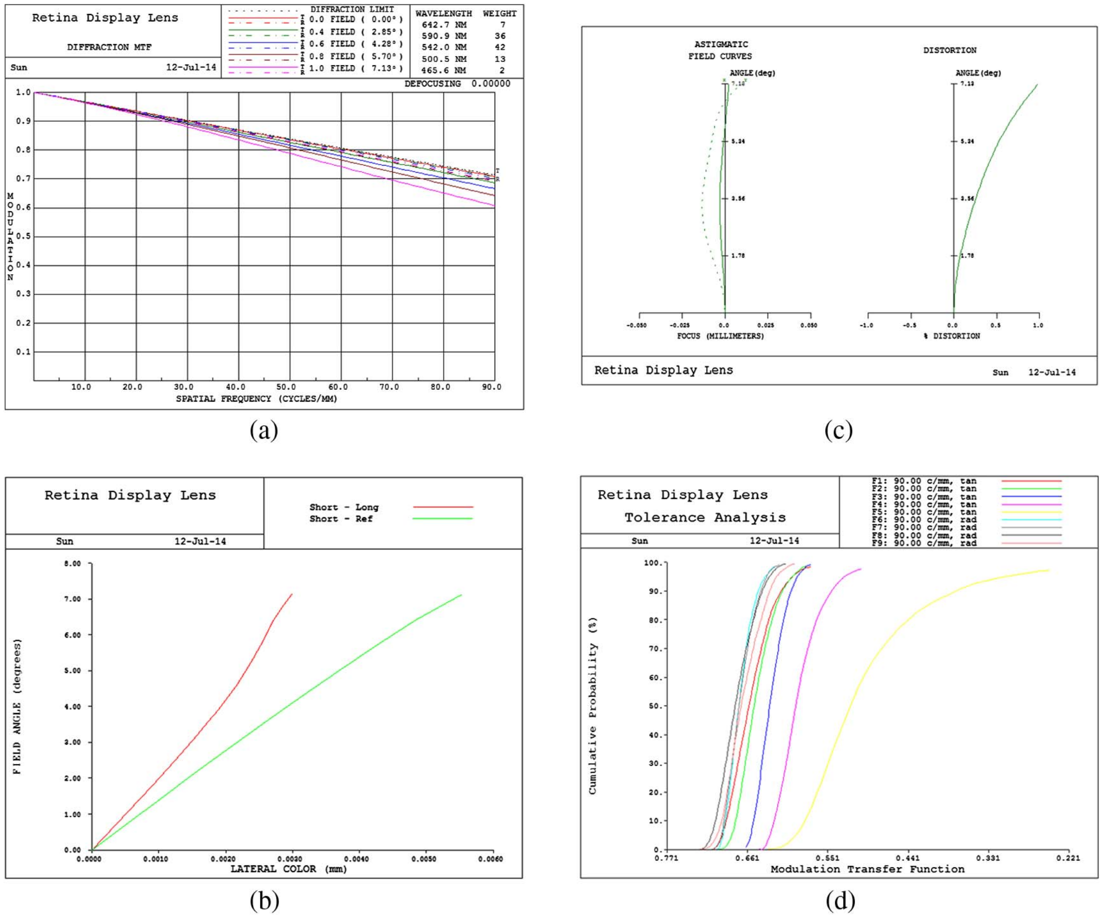

Fig. 3. Performance evaluation of the projection lens. (a) MTF curves for the half FOV of 0°–7.125°. (b) Lateral color. (c) Distortion and astigmatic field curves. (d) Tolerance analysis curves.

and the height is the radius ($D_{mia}/2$) of the lens unit, then the maximal angle can be calculated by

$$\tan(\theta_{\text{mlain}}) = \frac{D_{\text{mla}}}{2\,\text{EFL}} = \frac{n_{\text{mla}} D_{\text{mla}}}{2 f_{s1}}, \tag{2}$$

where D_{mla} is the diameter of the lens array unit, EFL is the effective focal length of the lens array, n_{mla} is the refractive index of the PMMA material, and f_{s1} is the focal length of the first surface.

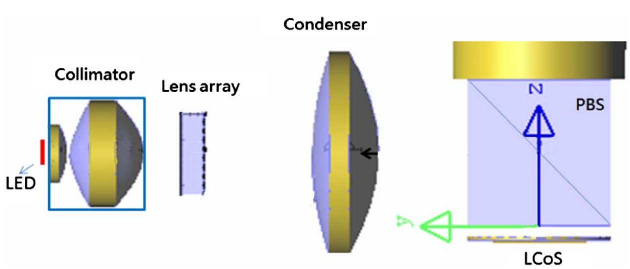

Fig. 4. Structure of the illumination system for the retinal projector.

D. Design of the Condenser

The design of the condenser is shown in Fig. 8. The aperture position of the condenser is the object focal point, making the condenser an image telecentric system. The lack of brightness at the assembly area and the edge of the illumination area should be taken into account in consideration of the illumination area. An overfill is added to make the image larger than the effective area of the LCoS. The image height h is set $= 1.3\ h_{\text{LCoS}}$ and is

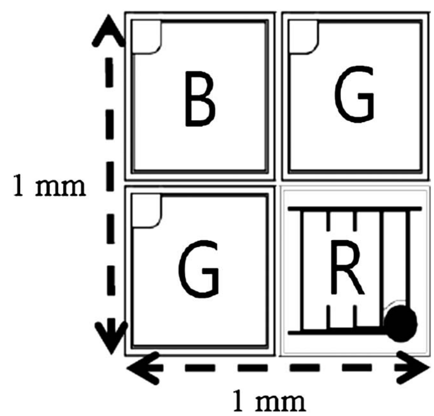

Fig. 5. LED chip layout.

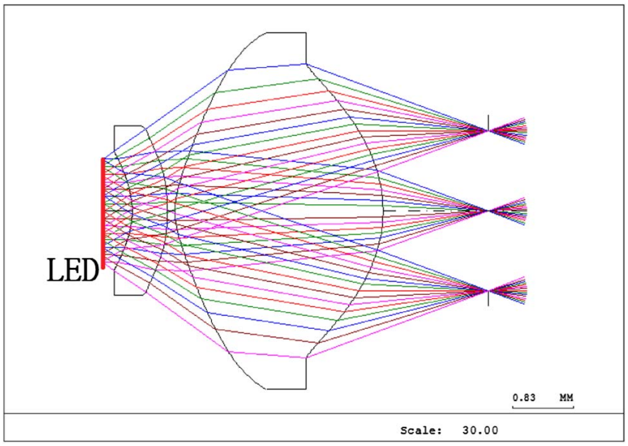

Fig. 6. Collimator layout.

Table 3. LED Specifications

Color	Wavelength (nm)	Type	Emission-pattern	Total flux (lm)
R	625	ODR20RF	Lambertian	9.42
G	525	ODT20RG	Lambertian	16
B	455	ODB20RG	Lambertian	3.45

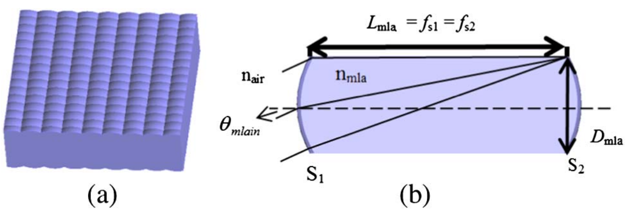

Fig. 7. Diagram of the lens array. (a) Lens array top view. (b) Lens array side view.

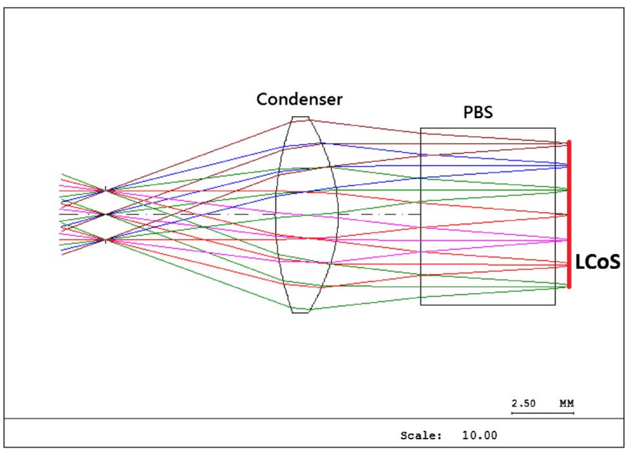

Fig. 8. Condenser and PBS layout.

larger than h_{LCoS}, which is the diagonal height of the effective area of the LCoS. If θ_{mlaout} is equal to θ_{mlain}, then the focal length of the condenser ($f_{condenser}$) can be obtained from the emission angle θ_{mlaout} and h as follows:

$$\tan\theta = \frac{h}{f_{condenser}}. \tag{3}$$

E. LCoS Panel Efficiency and Uniformity Analysis

Efficiency from the LED to the LCoS panel is the ratio of the luminous flux entering the effective area of the LCoS and the total luminous flux from the LED. The loss of luminous flux includes the transmittance loss from passing through the elements and the delivery loss between all elements. The delivery loss of an element can be calculated from the étendue, which is generally calculated by the Lambertian equation:

$$\text{étendue} = \pi A n^2 \sin^2(\theta), \tag{4}$$

where A is the area of the light-emitting surface or the receiving surface, θ is the receiving or emitting angle of the surface, and n is the refractive index of the medium. Table 4 shows the element efficiency and the cumulative efficiency for a Lambertian LED array. The receiving angle of the collimator is only 30°, and light from other angles is stopped by the collimator. The LED collection efficiency is 25%, as obtained from Eq. (4). The transmittance of each medium is set to be 98%; thus, the collimator efficiency is 92.24%, the lens array efficiency is 96.04%, the condenser efficiency is 92.24%, and the PBS efficiency is 48%. Energy loss from the LCoS is caused by the overfill, so that the receiving efficiency of the effective area of the LCoS is 59.17%, and the cumulative efficiency on the LCoS surface is revealed to be 5.80%. In the actual simulation, the efficiencies are 5.36% for the red LED, 5.51% for the green LED, 5.69% for the blue LED, and 5.48% for the white LED (RGB LED).

We next discuss the uniformity analysis. In this system, the eyepiece is located behind the panel so that the human eye can directly view the images on the LCoS panel through the ocular lens. In this case, the uniformity of the images viewed by the human eye can be evaluated by analyzing the uniformity of the illumination on the LCoS panel, as shown in Fig. 9. In addition, the uniformity is evaluated with ANSI/NAPM IT7.228-1997 and JBMA (Japanese standards). The extra idea of the mean deviation is introduced to show the uniformity of the system, as expressed in the following formula:

$$\text{Average Deviation} = \frac{\sigma}{\bar{x}}, \tag{5}$$

where σ is the standard deviation and $\bar{x}$ $\bar{x}$ is the mean of the data.

Table 4. Element Efficiency and Cumulative Efficiency

Item	Efficiency (%)	Cumulative Efficiency (%)
LED collection	25	25
Collimator	92.24	23.06
Lens array	96.04	22.15
Condenser	92.24	20.43
PBS	48	9.81
LCoS	59.17	5.80

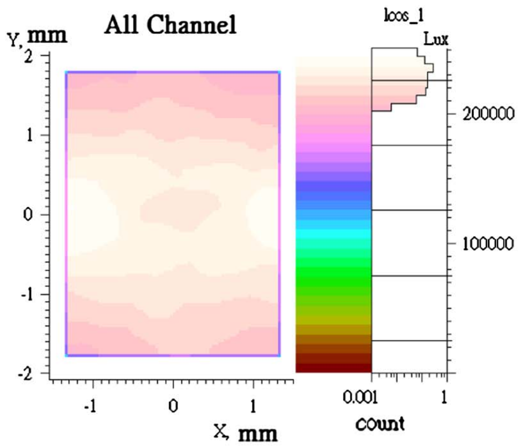

ANSI(+%)	-5.49%
ANSI(-%)	-9.51%
JBMA	92.31%
Average deviation	4.39%

(a)

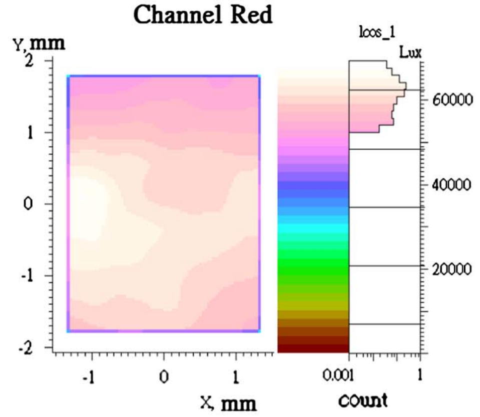

ANSI(+%)	-2.32%
ANSI(-%)	-10.89%
JBMA	93.38%
Average deviation	5.80%

(b)

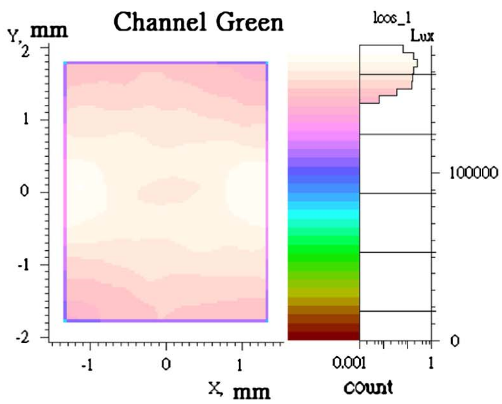

ANSI(+%)	-5.54%
ANSI(-%)	-10.41%
JBMA	92.28%
Average deviation	4.33%

(c)

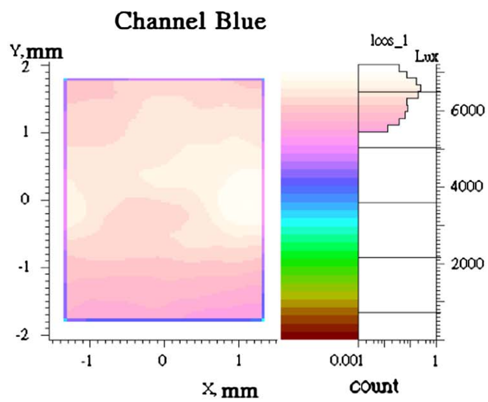

ANSI(+%)	-5.49%
ANSI(-%)	-9.51%
JBMA	92.31%
Average deviation	5.45%

(d)

Fig. 9. Simulation results for the uniformity. (a) All channels. (b) Red channel. (c) Green channel. (d) Blue channel.

To prevent the measurements from containing bias due to the use of specific points on the frame, sampling over the entire frame was used in the simulation to effectively evaluate the differences between each illumination block. A smaller value indicates greater uniformity of the illuminated area. We simulated the operation of the LED and performed a comparison of the uniformity of the LCoS panel. The simulation results for the emission uniformity of the all chips (white light), R chips (red light), G chips (green light), and B chips (blue light) are shown in Fig. 9. In comparison with general theater projectors, the JBMA uniformity is about 85%, revealing the favorable quality of the system.

5. ANALYSIS OF THE SEE-THROUGH RETINAL PROJECTOR

The eyepiece system and illumination systems were combined to form the optical system of the see-through retinal projector.

The human eye and color systems were also analyzed. Analysis for the human eye can be divided into analysis of the efficiency and the contrast ratio.

A. Efficiency Analysis at Human Eyes

For efficiency, consider a transmittance of the elements of 98%, the LCoS reflectance is 53%, and the BS reflectance is 50%. The estimated efficiency can be obtained from the difference between the illumination system $NA_{illumination}$ (0.122) and the eyepiece system NA_{image} (0.111). Definition of the NA ratio efficiency is expressed as follows:

$$\text{NA ratio efficiency} = \left(\frac{NA_{image}}{NA_{illumination}}\right)^2. \quad (6)$$

The NA ratio efficiency is calculated to be 82.78%. The light source is reflected by the LCoS to pass through the PBS, projection lens, and BD and then finally projected to the human eye. From the LCoS to the human eye, the cumulative efficiency is 18.66%, as shown in Table 5. The efficiency of 1.08% for the human eye is obtained by multiplying the coupling efficiency of 18.66% by the calculated LCoS panel efficiency of 5.8%. Simulated results are shown in Table 6.

B. Analysis of the Contrast Ratio at the Human Eye

A see-through system should consider the contrast ratio of the luminance between the eyepiece system image and the surrounding image in the eye. Thus, the equation can be expressed as follows:

$$\text{Contrast Ratio} = \frac{L_{eyepiece}}{L_{surroundings} \times T_{BS}}, \quad (7)$$

where $L_{eyepiece}$ is the luminance of the eyepiece system producing an image in the eye, T_{BS} is the transmittance of the BS, and $L_{surroundings}$ is the surrounding luminance.

With optical simulation for the luminance $L_{eyepiece}$, when all the chips emit, the display is 2.28×10^5 nit, and the transmittance T_{BS} of the BS is 50%. The chance in luminance of the surroundings is broad. When the luminance $L_{surroundings}$ for a horizontal view on a sunny day is about 2000 nit, the contrast ratio equals 228. When the luminance $L_{surroundings}$ such as when viewing the sky at a sunny day is about 20,000 nit, the contrast ratio is equal to 22.8. Apparently, the contrast ratio of the see-through retinal projection system can be adapted to high luminance from the surroundings. If the luminance is in the range of 200–800 nit, such as for the indoor lighting, then the contrast is in the range of 570–2280 nit.

Table 5. Efficiency Evaluation from LCoS to Human Eyes

Item	Efficiency (%)	Cumulative Efficiency (%)
LCoS reflectance	53	53
PBS	96.04	50.90
Projection lens	88.58	45.09
Beam splitter	50	22.54
NA ratio	82.78	18.66

Table 6. Efficiency for Human Eye

Item	Efficiency (%)
Evaluate value	1.08
All channels	0.97
Red channel	0.97
Green channel	0.97
Blue channel	0.97

C. Color Analysis of the Retinal Projection System

The color system [15,16] of the retinal projector utilizes a color sequence achieved by LED color chips. The LED spectrum can be used to calculate the x and y values of the color coordinates of the color chips. The x and y coordinates in the term (x, y) are (0.687, 0.313) for the red LED (0.142, 0.776) for green, and (0.148, 0.028) for blue, respectively.

A triangular NTSC color gamut [17] can be drawn as a CIE 1931 x–y chromaticity diagram. The ratio obtained by dividing the triangular area of the LED color gamut for this system by the triangular NTSC color gamut is used to evaluate the color performance of the system, as shown in Fig. 10. The white line indicates the color gamut of the retinal projector. This system reveals a 128% NTSC color gamut.

D. System Design for the Camera

A camera is included in the design to acquire external images for effective interaction with users. A CMOS with a 30° half

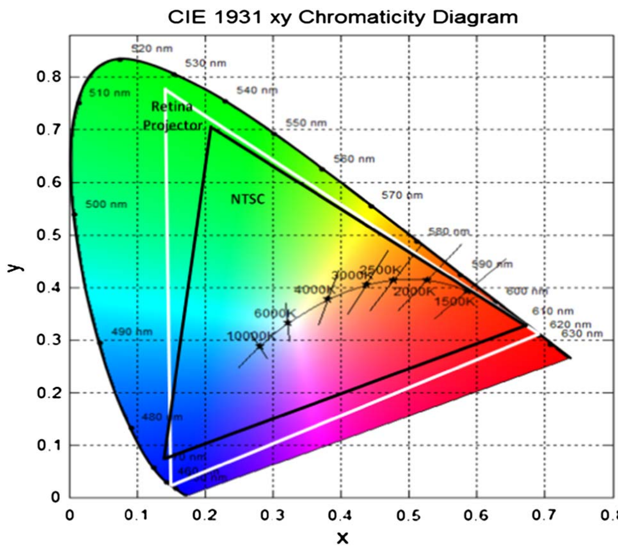

Fig. 10. Color gamut of the retinal projector.

Table 7. First-Order Data for the Camera

Specifications	Value
Sensor type	OV2643 (CMOS)
Array size	1600 × 1200 (UXGA)
Pixel size	2.2 μm × 2.2 μm
Image size	3.52 mm × 2.64 mm
Half-FOV	30°
EFL	3.81 mm
F/#	2.8
Chief ray angle	<25°

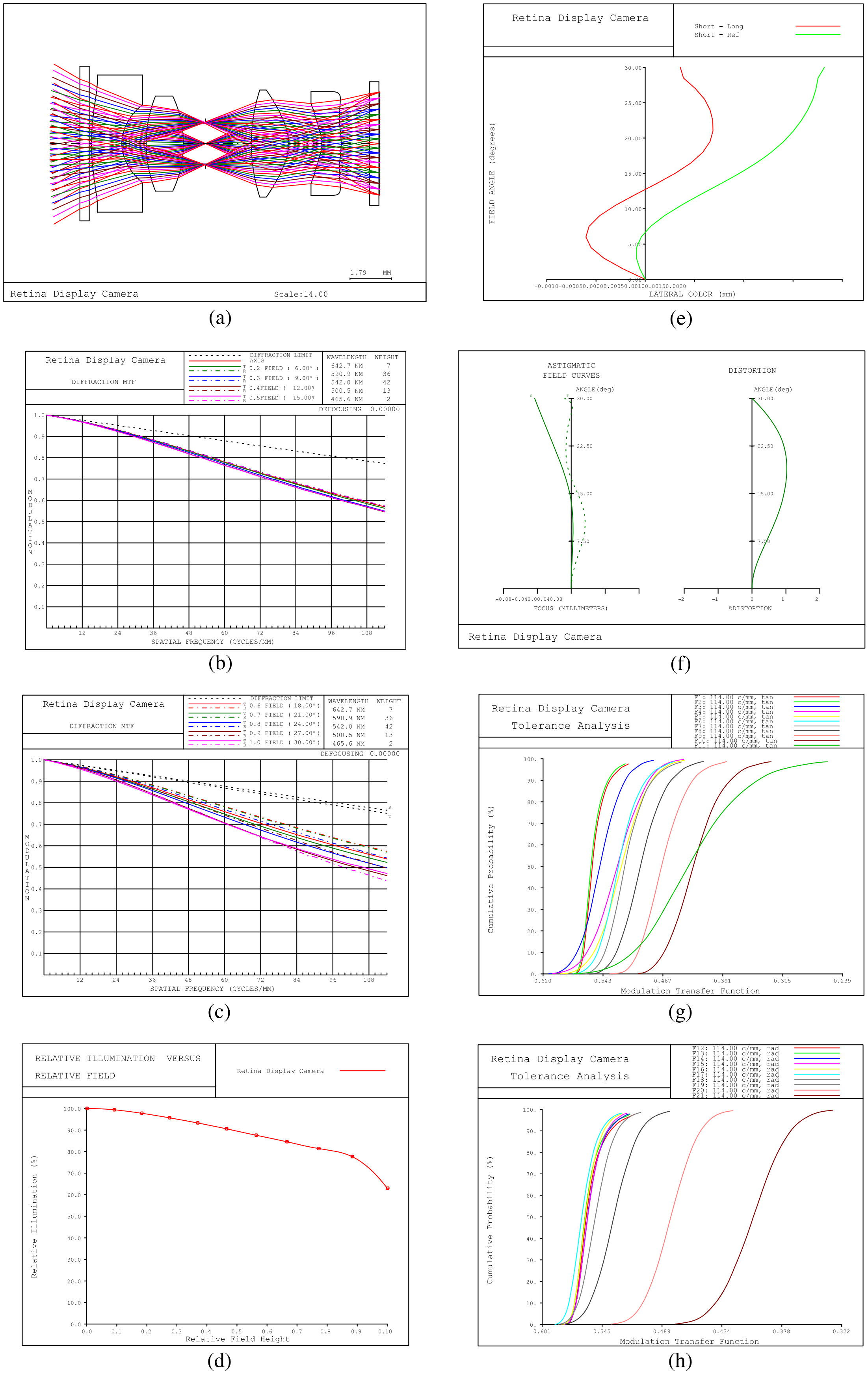

Fig. 11. Performance evaluation of the camera. (a) Optical system layout. (b) MTF curves for half FOV of 0°–5°. (c) MTF curves for half FOV of 18°–30°. (d) Relative illumination. (e) Lateral color. (f) Distortion and field curves. (g) Tangential tolerance analysis. (h) Radial tolerance analysis.

FOV, F/2.8 aperture, and 2 million pixel resolution is selected for the design, and the first-order specifications are presented in Table 7. The retinal projector with a 7.125° half FOV causes the outer image to overlay the panel image and forms an image in the eye. However, normally, human memory cannot retain a detailed image after seeing a scene, and it is difficult to remember the image in detail for a long period of time. The digital camera has a half FOV of 30°, four times greater than the viewing angle of the retinal projector. The projector can be locally enlarged to the field of view of the retinal projector. The digital camera has a large viewing angle for capturing images of the surrounding scene, which can be stored for a long time.

To preserve the four lightweight plastic lens pieces, a protective glass lens and IR filter are used, as shown in Fig. 11. Figure 11(a) shows the composition of the lenses, and Fig. 11(b) presents the relations between MTF and the spatial frequency. The MTF curve with a half FOV of 0°–15° is larger than 54% at 0–114 lp/mm. Figure 11(c) shows the MTF curve with a half FOV of 18°–30°, which is larger than 43% at 0–114 lp/mm. Figure 11(d) reveals the relations between the relative luminance and the FOV. The maximal FOV is 63%. Figure 11(e) presents the relations between the lateral color and the FOV, where the longitudinal chromatic aberration curve from 465.61 to 642.73 nm is indicated by a red line, with the maximum being 0.69 μm; the green line indicates the longitudinal chromatic aberration curve from 465.61 to 542.02 nm, with the maximum being 1.82 μm. Figure 11(f) shows the relations between the distortion and the FOV, where the maximal distortion is 1% and the TV distortion is 1%, and indicates the distortion and difference in the FOV between 0.6 and 1.0. Figure 11(g) presents the tangential tolerance analysis.

Table 8. Weight Analysis of the Image System

Item	Volume (mm^3)	Material	Specific Gravity	Weight (g)
Beam splitter	36.64	NBK7	2.51	0.092
Lens 1	275.56	POLEFINH	0.95	0.276
Lens 2	282.56	Z-E48R	1.01	0.283
Lens 3	263.07	OKP4	1.22	0.321
Total				0.972

Table 9. Weight Analysis of the Illumination System

Item	Volume (mm^3)	Material	Specific Gravity	Weight (g)
PBS	195.11	SF11	3.22	0.628
Condenser	84.85	PMMA	1.18	0.100
Lens array	7.03	PMMA	1.18	0.008
Collimator 1	27.10	Z-E48R	1.01	0.027
Collimator 2	6.80	PEIO	1.27	0.009
LED		RGB LED Array		0.500
LCoS		0.17 in. (0.4318 cm) LCoS		3.500
Total				4.772

Table 10. Weight Analysis of 2 Megapixel Digital Camera

Item	Volume (mm^3)	Material	Specific Gravity	Weight (g)
Protection glass 1	19.47	NBK7	2.51	0.049
Lens 1	106.56	"POLEFINH"	0.95	0.101
Lens 2	19.01	"POLEFINH"	0.95	0.018
Lens 3	12.30	"POLEFINH"	0.95	0.012
Lens 4	48.22	"PEIO"	1.27	0.061
IR filter	13.55	NBK7	2.51	0.034
Total weight				0.275

It can be seen that the tolerance MTF of all fields of view is larger than 30% at 114 lp/mm and the cumulative probability is 97.7%. Figure 11(h) shows the radial tolerance analysis results. It can be seen that the tolerance MTF of all fields

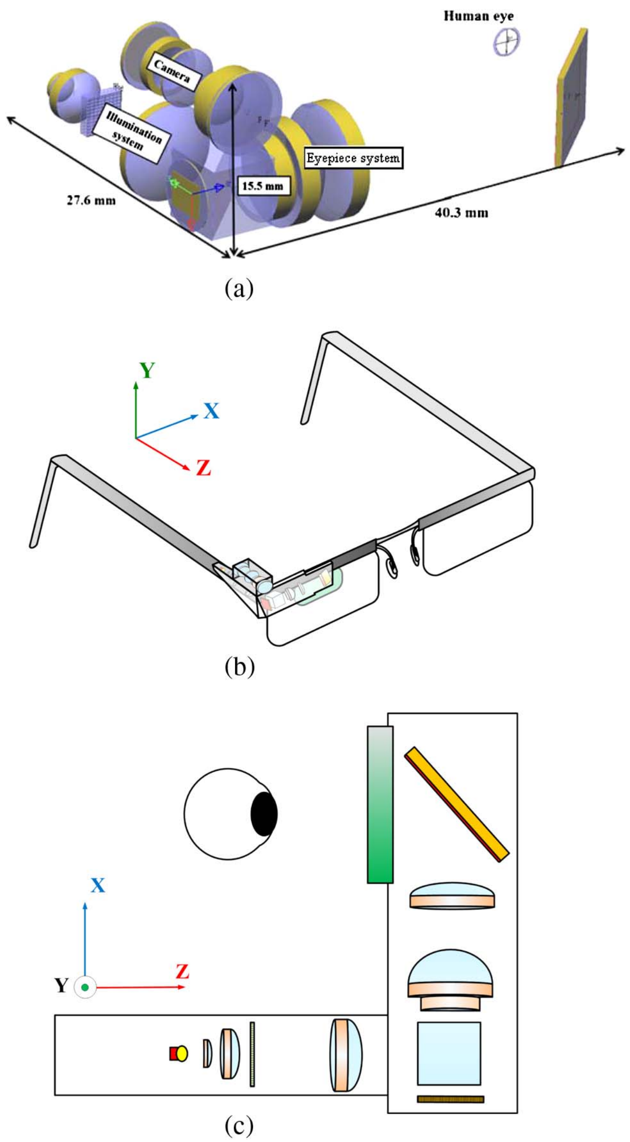

Fig. 12. Design schemes of the retinal projector. (a) Side view of the system. (b) Diagram of the eyeglasses. (c) Top view of the eyeglasses.

of view is larger than 35% at 114 lp/mm when the cumulative probability is 97.7%.

E. Weight and Volume Analyses of the Retinal Projection System

The retinal projection system is a type of head-mounted display in which comfort needs to be taken into account. Volume and weight can directly affect the user; therefore, both are analyzed to ensure they are suited to the user's needs. The weight of the eyepiece system is 0.972 g (as shown in Table 8), the weight of the illumination system is 4.772 g (Table 9), and the weight of the camera is 0.275 g (Table 10); therefore, the total weight is 6.02 g. The weight of regular glasses is about 20–50 g and could be even heavier depending on the prescription. The total system should allow users to have a comfortable experience.

The volume of the system is 40.3 mm × 27.6 mm × 15.5 mm, and the total volume of the optical system is about 5.83 cm × 5.83 cm × 5.83 cm, which is more compact than previous devices. Compared to current head-mounted displays on the market, this can be regarded as a mini system. Design schemes of the retinal projector combined with eyeglasses are shown in Fig. 12.

6. CONCLUSIONS

The decreased size and weight of the optical system is critical for use in head-mounted displays. In this work, a wearable, lightweight, see-through retinal projector with an optical camera system is designed. The weight of the projector imaging system is 0.972 g, the weight of the illumination system is 4.772 g, and the weight of the camera system is 0.275 g to obtain a total weight of 6.02 g. The total volume of the optical system is about 5.83 cm^3. With a 0.177 in. (0.44958 cm). VGA LCoS panel, a 20 in. (50.8 cm) upright virtual image is displayed 2 m in front of the eye, with an emitting half FOV of 7.125°, exit pupil diameter of 4 mm, and eye relief of 10 mm. The imaging quality of the projector reveals an MTF larger than 60% at a spatial frequency of 90 lp/mm, the distortion less than 0.98%, TV distortion less than 0.63%, and the lateral color less than 5.6 μm. The tolerance analysis shows that the MTF of all fields of view is larger than 31%. The uniformity of the illumination system is larger than 92.28% in the JBMA, the mean deviation is less than 5.8%, and the cumulative efficiency is 5.80% for the LCoS surface. The human eye efficiency of the projection system is 0.78%, the contrast ratio presents at least 228 in the horizontal field, and the gamut space of the system is 128% NTSC color gamut. Finally, the camera has a 30° half angle of view and an aperture of F/2.8 with a resolution of 2 million pixels. The image quality reveals that the MTF of all fields of view is larger than 40% at a spatial frequency of 114 lp/mm, the distortion is less than 1%, the TV distortion is less than 1%, the lateral color less than 2.2 μm, and the MTF of all fields of view larger than 30%, according to the tolerance analysis.

Ministry of Science and Technology of Republic of China, Taiwan (MOST 103-2221-E-008-052, MOST 103-2622-E-035-023-CC3).

REFERENCES

1. I. E. Sutherland, "A head-mounted three dimensional display," in *American Federation of Information Processing Societies '68, Proceedings of Fall Joint Computer Conference*, (Association for Computing Machinery, 1968), pp. 757–764.
2. F. J. Ferrin, "Current issues in helmet mounted display systems for military applications," Proc. SPIE **3362**, 71–79 (1998).
3. O. Cakmakci and J. Rolland, "Head-worn displays: a review," J. Disp. Technol. **2**, 199–216 (2006).
4. J. Wilson, D. Steingart, R. Romero, J. Reynolds, E. Mellers, A. Redfern, L. Lim, W. Watts, C. Patton, J. Baker, and P. Wright, "Design of monocular head-mounted displays for increased indoor firefighting safety and efficiency," Proc. SPIE **5800**, 103–114 (2005).
5. J. P. Rolland, F. Biocca, F. Hamza-Lup, Y. Ha, and R. Martins, "Development of head-mounted projection displays for distributed, collaborative, augmented reality applications," Presence **14**, 528–549 (2005).
6. R. Kijima and M. Hirose, "A compound virtual environment using the projective head mounted display," in *Proceedings of International Conference on Virtual Reality Software and Technology* (IEEE, 1995).
7. R. W. Fisher, "Head-mounted projection display system featuring beam splitter and method of making same," U.S. patent 5,572,229 (Nov. 5, 1996).
8. J. L. Fergason, "Optical system for a head-mounted display using a retro-reflector and method of displaying an image," U.S. patent 5,621,572 (Apr. 15, 1997).
9. J. E. Melzer, F. T. Brozoski, T. R. Letowski, T. H. Harding, and C. E. Rash, "Guidelines for HMD design," in *Helmet-Mounted Displays: Sensation, Perception and Cognition Issues* (U.S. Army Aeromedical Research Laboratory, 2009), pp. 805–848.
10. J. P. Rolland and H. Fuchs, "Optical versus video see-through head-mounted displays in medical visualization," Presence **9**, 287–309 (2000).
11. A. A. Cameron, "Optical waveguide technology and its application in head mounted displays," Proc. SPIE **8383**, 83830E (2012).
12. J. P. Rolland, K. P. Thompson, H. Urey, and M. Thomas, "See-through head worn display (HWD) architectures," in *Handbook of Visual Display Technology*, J. Chen, W. Cranton, and M. Fihn, eds. (Springer, 2012), pp. 2146–2170.
13. A. Bauer and J. P. Rolland, "Visual space assessment of two all-reflective, freeform, optical see-through head-worn displays," Opt. Express **22**, 13155–13163 (2014).
14. J. W. Pan, S. H. Tu, C. M. Wang, and J. Y. Chang, "High efficiency pocket-size projector with a compact projection lens and a light emitting diode-based light source system," Appl. Opt. **47**, 3406–3414 (2008).
15. G. Wyszecki and W. S. Stiles, *Color Science: Concepts and Methods, Quantitative Date and Formulas*, 2nd ed. (Wiley, 1982).
16. R. S. Berns, *Billmeyer and Saltzman's Principles of Color Technology*, 3rd ed. (Wiley, 2000).
17. Wikipedia, Gamut, http://en.wikipedia.org/wiki/Gamut.